CONTROL AND POINTING CHALLENGES OF THE NASA DEEP SPACE NETWORK ANTENNAS

WODEK GAWRONSKI

Jet Propulsion Laboratory, California Institute of Technology, Pasadena, CA 91109, U.S.A,
Wodek.K.Gawronski@jpl.nasa.gov

Abstract. The paper presents the problems in precision pointing of the NASA Deep Space Network (DSN) antennas, and measures taken to minimize their impact on pointing accuracy.

Key Words: antennas, control systems, pointing, tracking

1. NASA DEEP SPACE NETWORK

The NASA Deep Space Network antennas serve as a communication tool for the NASA deep space missions. The antennas located at Goldstone (California), Madrid (Spain), and Canberra (Australia) assure continuous tracking of spacecraft during Earth rotations. They track spacecraft receiving spacecraft RF signal (downlink), or sending the signals to spacecraft (uplink). The signal frequency is either 8 GHz (X-band), or 32 GHz (Ka-band). The dish size of the antennas is either 34 meters or 70 meters. An example of the 34-meter antenna is shown in Fig.1. The antenna dish rotates with respect to horizontal axis (called elevation axis). The whole antenna structure rotates on wheels rolling on a circular track (azimuth track) with respect to the vertical axis (called azimuth axis).

In order to maintain communication with a spacecraft at Ka-band the ground antennas must track with precision of order of 1 millidegree. This requirement is rather demanding for antennas of this size. In order to meet it, the antenna structural design, instrumentation, and control system shall be revisited. This paper describes some of the recent upgrades in the antenna structure, control system, and instruments that improve its pointing accuracy.
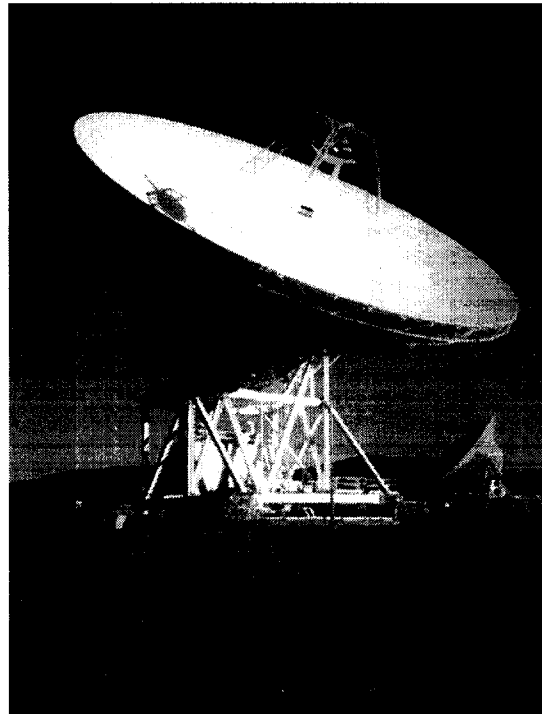

Figure 1. 34-meter antenna at Goldstone, California, with 70-meter antenna behind it.

2. POINTING ERROR SOURCES

The following factors impact antenna pointing precision:

1. Azimuth track level unevenness.
2. Wind gusts disturbances.
3. Large antenna movements that cause actuator saturation.
4. Mechanical imperfections (such as axis orthogonality, dish panel imperfect adjustment, or encoder imperfections).
5. Deformations of the antenna structure due to thermal gradient.
6. Antenna model imperfections (for controller design).
7. Deformation of the antenna dish due to gravity.
8. Atmospheric diffraction.
9. Dry friction of wheels on track.
10. Gearbox backlash.
11. Other systematic errors of unknown origin.
12. Random errors of unknown origin.
13. Non-collocation of the sensors (encoders) and the RF beam position, and non-collocation of the actuators (torque) and disturbance (wind pressure).

3. SOLUTIONS

The following measures address the pointing problems and reduce pointing errors:

1. Alidade deformations due to the AZ track level unevenness: implementing look-up table, see [3].
2. Wind disturbances: improved control algorithms (including antenna models), see [1], [4], [5], [7], [10], [11], [12], [13], and [14].
3. Large displacement with actuator saturation: applying command preprocessor, see [2].
4. Dish deformations: using lasers, holography, or adjustable panels for correction.
5. Thermal deformations: installation of temperature sensors, and/or thermal insulation.
6. Model imperfections: performing system identification to obtain an accurate model, [10].
7. Dish gravity deformations: use a look-up table, or apply small mirror deformations.
8. Atmospheric diffractions: use weather updates every 1 sec.
9. Dry friction of wheels and track: apply dither to the drives, see [9].
10. Backlash in gearboxes: use dual motors with counter-torque, see [6].
11. Unknown systematic errors: use tests to create a look-up table.
12. Random errors: use monopulse control, see [8], or conical scan (conscan), see [15].
13. Non-collocation of inputs and outputs – no solution.

4. DETAILS OF SELECTED SOLUTIONS

We present more details on items 1, 2, 3, 6, 12.

4.1. Models

In the antenna design stage analytical models of the open-loop antenna (which includes structure and drives) are used. The open-loop model is shown in Fig.2. It consists of the antenna structure and drives connected by the rate feedback loops. The structure model is obtained from the finite element code, its size reduced in modal coordinates using the controllability and observability grammians and transferred to Simulink. The drive models are modeled with Matlab/Simulink.

Antenna model used in the controller algorithm is obtained from field tests and system identification. White noise signal is applied at the input (AZ rate or EL rate) and the antenna response is measured at AZ encoder or EL encoder, respectively. Samples of the input and output signals are shown in Fig.3, and magnitudes of the antenna transfer function obtained from the field data and from the identified model are compared in Fig.4.
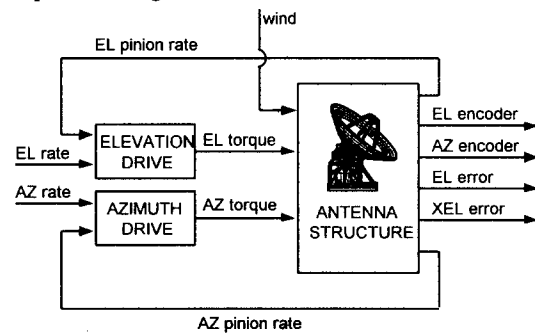

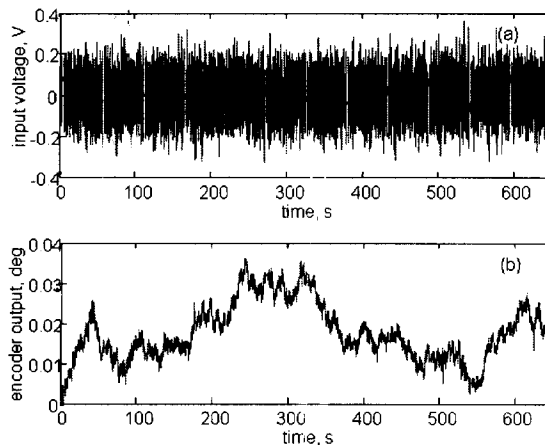**Figure 2.** Antenna open-loop or (rate-loop) model

Figure 3. Input (a) and output (b) signals used in the system identification procedure

4.2. Control Algorithms

Antenna controls system consists of the rate and position loops. The rate loop uses tachometer feedback, see Fig.2, while the position loop uses encoder feedback, see Fig.5. The PI, LQG, and H$_\infty$ control algorithms are used in the position loop.

The simplest one, PI controller, is shown in Fig.6, and its performance is illustrated in Fig.7. The

antenna settling time with PI controller is 18 s, its bandwidth is 0.1 Hz. It has also low disturbance rejection properties.
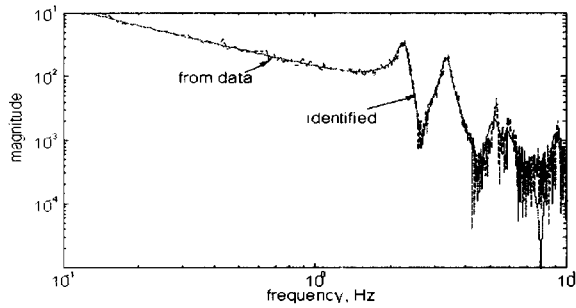

Figure 4. Magnitudes of the antenna transfer function: obtained from field data (dashed line), and from the identified model (solid line).
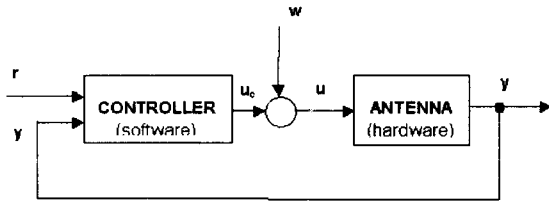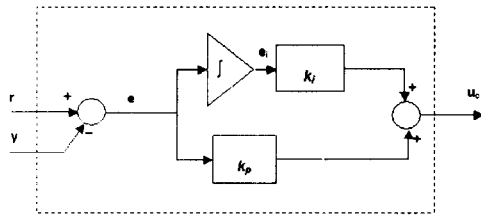

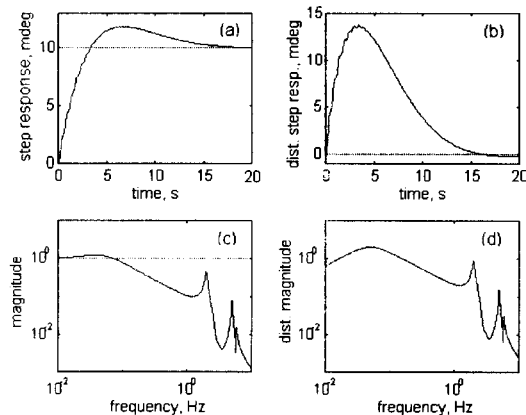**Figure 5** Antenna closed-loop system

Figure 6. PI controller

Figure 7. Antenna performance with PI controller

The LQG controller is shown in Fig.8. It is model-based controller, since it includes an estimator. The estimator equations include antenna

model, which has to be accurate in order to preserve stability of the closed-loop system. The antenna model from system identification is used in the estimator.

The performance of the LQG controller is illustrated in Fig.8. Its settling time is 2 s, its bandwidth is 2 Hz, and the wind disturbance rejection properties improved 10 fold with respect to the PI controller.
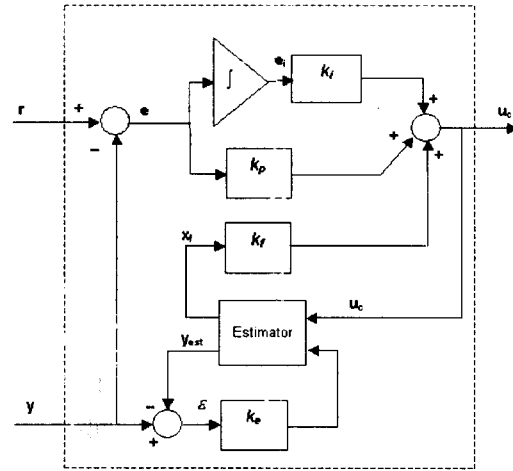

Figure 8. LQG and H_∞ controllers
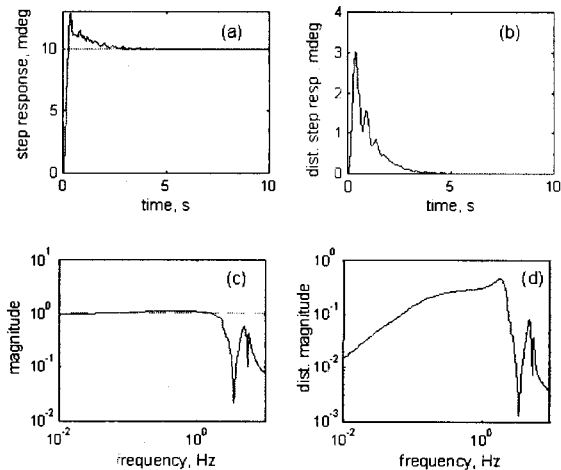

Figure 9. Antenna performance with LQG controller

The H_∞ controller performance is shown in Fig.10. It has settling time less than 1 s, extended bandwidth, and the wind disturbance rejection properties improve 10 fold with respect to the LQG controller.

4.3. Command Pre-Processor

Antenna dynamics are restricted by the imposed rate limit (0.8 deg/s) and acceleration limit (0.4 deg/s^2). In order to avoid rate and acceleration

3

saturation (that cause limit cycling) a command preprocessor (CPP) is implemented
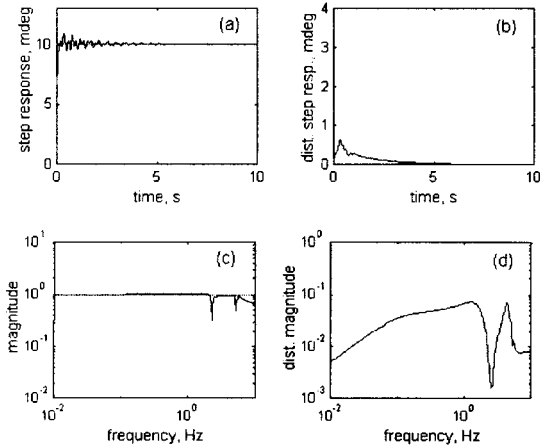

Figure 10. Antenna performance with H∞ controller

CPP is a piece of software that performs operations illustrated in Fig.12. It simulates the dynamics of a rigid antenna. The rate and acceleration are limited; and, it is controlled using the feedforward gain, and PD controller with variable P and D gains. The P gain depends on the CPP error, and D gain depends on the CPP error derivative, as shown Fig.13.
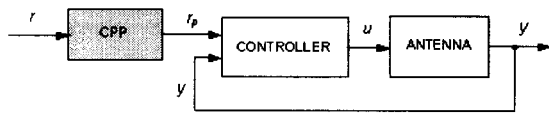

Figure 11. Location of CPP in the control system
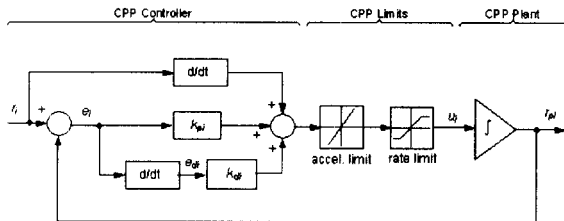

Figure 12. The CPP structure

The antenna responses to 10 deg step shown in Fig.14a for the antenna with CPP, and in Fig.14b for the antenna without CPP show that CPP eliminates limit cycling.
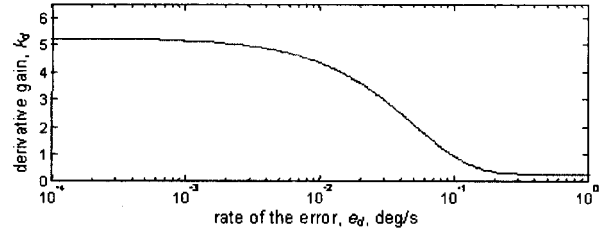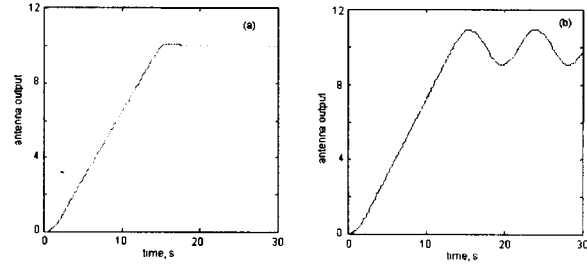

Figure 13. The CPP derivative gain

Figure 14. Antenna response to 10 deg step: (a) with CPP, and (b) without CPP

4.4. AZ Track Imperfection

The wheel-and-track rotation system is implemented to rotate the antenna in azimuth (i.e. with respect to its vertical axis). The track profile was measured using inclinometers and Fig.15 shows that the track is not perfectly flat. The inclinometer locations on the antenna lower structure (alidade) are shown in Fig.16.

The inclinometers measured antenna tilts in x- and y-directions during the antenna clockwise and counter-clockwise rotations by 360 deg. The sample of measurements of the antenna tilts with respect to x-axis is shown in Fig.17. From the measurements we extracted a sinusoidal component that reflected the tilt of the antenna azimuth axis, see Fig.17.

The tilts were used to create the look-up table to correct the antenna pointing. The effectiveness of the correction is shown in Fig.18.
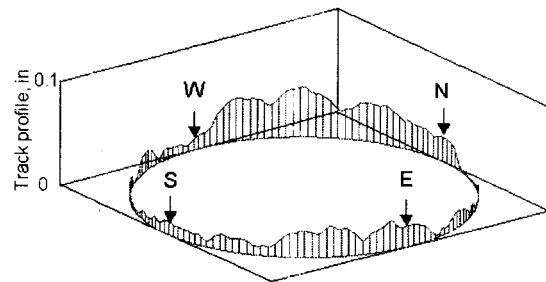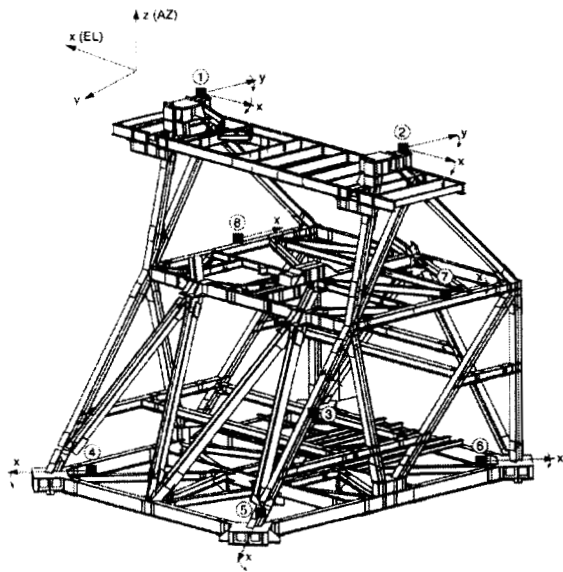

Figure 15. Track profile, inches.

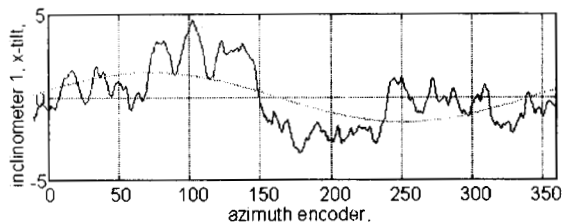**Figure 16.** Inclinometer locations on the alidade.
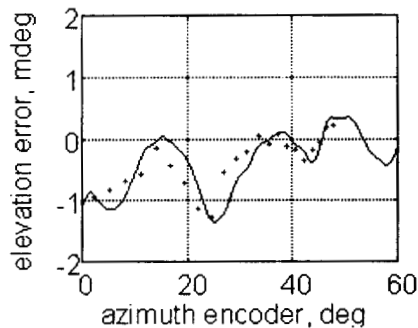

Figure 17. Antenna tilts, *x*-axis

Figure 18. Elevation pointing errors obtained from the azimuth correction table (solid line), and from the conscan measurements (dots)

Additionally, tilts were measured for a stationary antenna during 48-hour period. The *y*-tilts are shown in Fig.19. They represent the antenna thermal deformations. Note that they are more intense afternoon.
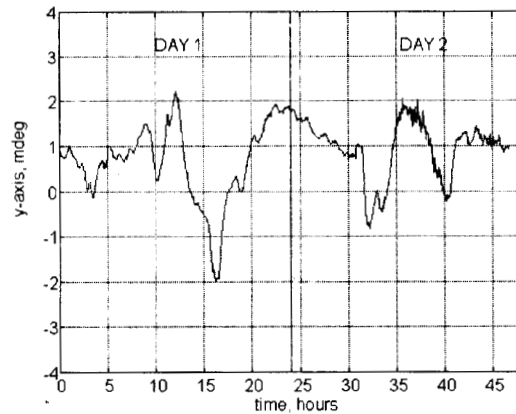

Figure 19. Antenna tilts due to temperature gradient.

4.5. Conscan

Random (unpredictable) errors are compensated using the conical scanning (conscan) technique. In this approach an antenna (during tracking) performs additional circular motion, see Fig.20. The power of the received signal depends on the antenna position with respect to the boresight, as shown in Fig.21.
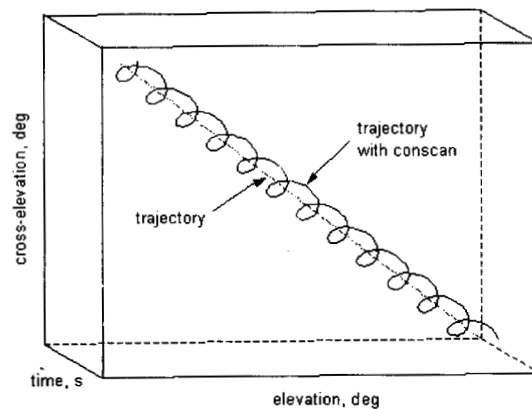

Figure 20. Antenna conical scanning motion.

During conical scanning, when the antenna is on target the receiving power is constant, c.f. Figs. 21 and 22. However, if the antenna is off-target, the power varies in a sinusoidal pattern. The amplitude and phase of the sinusoid allows to estimate the target position and to close the conscan feedback loop. The disturbance rejection property of this feedback is illustrated in Fig.23.
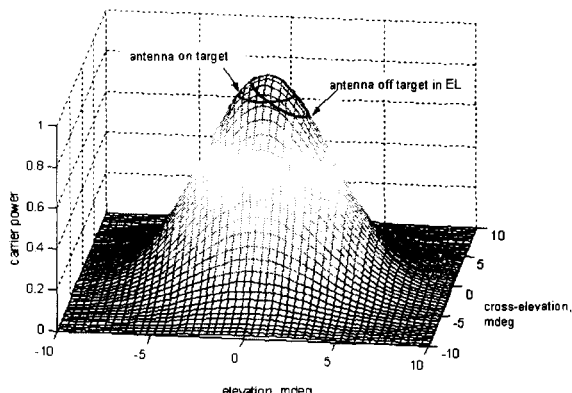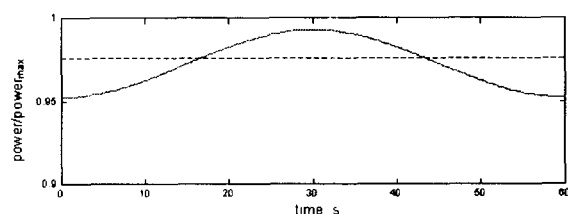
5

Figure 21. Antenna receiving power

Figure 22. Antenna on target (dashed line), and off-target (solid line).
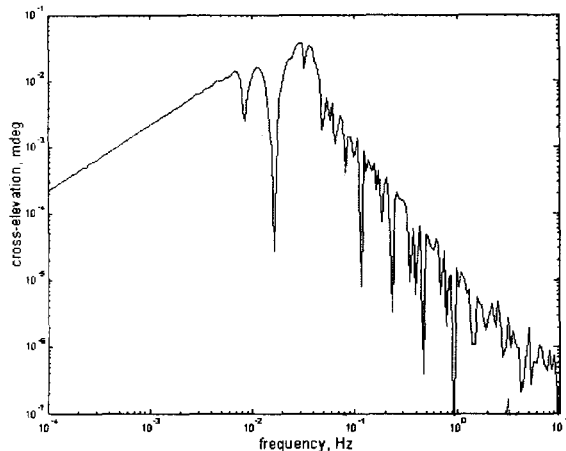

Figure 23. Estimation error in response to elevation harmonic disturbance of amplitude 0.1 mdeg

5. CONCLUSIONS

We presented various aspects of the antenna control and pointing problems, along with their solutions. Additional solutions, not presented in this paper, can be found in the JPL Interplanetary Network Progress Reports, available at the following web-page address: http://tmo.jpl.nasa.gov/tmo/progress_report/

REFERENCES

1. Gawronski W., Bienkiewicz B., and Hill R.E.: Wind-Induced Dynamics of a Deep Space Network Antenna, Journal of Sound and Vibration, vol.178, No.1, 1994.
2. Gawronski W., and Almassy W.: Command Preprocessor for Radiotelescopes and Microwave Antennas. IEEE Antennas and Propagation Magazine, vol.44, No.2, 2002.
3. Gawronski W., Baher F., and Quintero O.: Azimuth Track Level Compensation to Reduce Blind Pointing Errors of the Deep Space Network Antennas, IEEE Antennas and Propagation Magazine, vol.42, No.2, 2000.
4. Gawronski W.: Antenna Control Systems: from PI to H_∞, IEEE Antennas and Propagation Magazine Vol.43, No.1, 2001
5. Gawronski W., and Mellstrom J.A.: Control and Dynamics of the Deep Space Network Antennas, in: Control and Dynamics Systems, ed. C.T. Leondes, vol. 63, Academic Press, San Diego, 1994, pp. 289-412.
6. Gawronski W., Beech-Brandt J.J., Ahlstrom H.G., Jr., and Maneri, E.: Torque-Bias Profile for Improved Tracking of the Deep Space Network Antennas. IEEE Antennas and Propagation Magazine, vol.42, No.6, 2000.
7. Maneri E., and Gawronski W.: LQG Controller Design Using GUI: Application to Antennas and Radio-Telescopes, ISA Transactions, 2000
8. Gawronski W., and Gudim M.A.: Design and Performance of the Monopulse Control System, IEEE Antennas and Propagation Magazine, 1999.
9. Gawronski W., and Parvin B.: Radiotelescope Low Rate Tracking Using Dither, AIAA Journal of Guidance, Control, and Dynamics, vol.21, 1998.
10. Gawronski W., Racho C., and Mellstrom J.: Application of the LQG and Feedforward Controllers for the DSN Antennas, IEEE Trans. on Control Systems Technology, vol.3, 1995.
11. Gawronski W.: A Balanced LQG Compensator for Flexible Structures, Automatica, No 10, 1994.
12. Gawronski W.: Design of a Linear Quadratic Controller for the Deep Space Network Antennas, AIAA Journal of Guidance, Control, and Dynamics, vol.17, 1994.
13. Gawronski W.: Predictive Controller and Estimator for NASA Deep Space Network Antennas, ASME Transactions, Journal of Dynamic Systems, Measurements, and Control, No2, 1994.
14. Gawronski W., and Mellstrom J.A.: Antenna Servo Design for Tracking Low-Earth-Orbit Satellites, AIAA Journal of Guidance, Control, and Dynamics, vol.17, 1994.
15. Gawronski W., and Craparo E.M.: Three Scanning Techniques for DSN Antennas to Estimate Spacecraft Position, Interplanetary Network Progress Report, vol.42-147, 2001.

6